

# ZnO-Cu<sub>2</sub>O Composites for Photocatalytical Removal of Methylene Blue from Aqueous Solution under Visible Light

Nasrin Akter, Mahbuba Zaman, Md. Aatur Rahman and Md. Mufazzal Hossain\*

*Department of Chemistry, University of Dhaka, Dhaka 1000, Bangladesh*

(Received: 3 October 2022; Accepted: 31 January 2023)

## Abstract

ZnO-Cu<sub>2</sub>O composites were prepared by precipitation technique followed by calcination. The prepared composite was characterized by scanning electron microscopy (SEM), energy dispersion X-ray (EDX), Fourier transform infra-red (FT-IR) and X-ray diffraction (XRD). Band gap energy of the composite was determined by UV-visible reflectance measurement. The absorption range of the ZnO-Cu<sub>2</sub>O composite was shifted to the visible region due to the doping of Cu<sub>2</sub>O. SEM image represented that composite nanoparticle was smaller in size compared to the pure ZnO. The EDX spectral analysis showed that no elements other than Zn, Cu and O were present in the sample. XRD showed that ZnO-Cu<sub>2</sub>O composite was made of hexagonal ZnO and cubic Cu<sub>2</sub>O. The photocatalytic activity of ZnO-Cu<sub>2</sub>O composite was studied by degrading MB under different experimental conditions. The molar ratios of the composites, amount of the composite, initial concentration of dyes were varied to optimize the conditions for degradation. The experimental result was compared with those of commercial ZnO. It was found that the ZnO-Cu<sub>2</sub>O composite is a better photocatalyst than ZnO under visible light.

**Keywords:** ZnO-Cu<sub>2</sub>O composite, methylene blue, photocatalytic activity, doping

## I. Introduction

Direct discharge of effluents into water streams from the textile and leather industries contains a significant amount of cancer-causing and nonbiodegradable dyes. Methylene blue (MB) is used for temporary hair dyeing, coloring paper stock, coloring cotton and wool, and coloring paper<sup>1</sup>. The proper treatment of wastewater containing dyes is one of the hardest challenges facing the manufacturing industry today. Due to the hazardous effects, it is highly undesirable to dump industrial wastewater containing dye into bodies of water. MB may be released into the environment through several waste streams as a result of its production and use as a cosmetic dye, chemical intermediary, medicinal agent, paper dye, microscope stain, and dye for paper. To treat the effluent from the textile dyeing industries, a variety of physical processes and chemical methods were developed. Organic contaminants, including dyes, can be effectively removed using physical methods such as adsorption utilizing activated carbon. Reactivating the adsorbent for reuse is not cost-effective in industrial applications. The techniques involving membrane filtration have the potential to completely remove the dyes and produce re-used water. But all physical methods eventually result in the production of secondary waste<sup>2</sup>. Some kinds of dyes are decoloured via chemical procedures such as ozonation, sodium hypochlorite treatment, and electrochemical destruction. However, ozone must first be prepared onsite before being used in ozonation. Water treated with hypochlorite has a high chloride concentration, and electrochemical destruction takes a lot of electricity, which is not practical from an economic standpoint. The semiconductor-based photocatalytic process has been widely applied in recent years as a promising and

efficient method to address the world's concerns with organic pollution and energy. There are typical photocatalyst such as TiO<sub>2</sub>, ZnO, and WO<sub>3</sub> etc. The majority of them can respond to ultraviolet (UV) light, despite the fact that UV light makes only about 3% to 5% where visible light is 43% in nature<sup>3</sup>. Consequently, it is essential<sup>4</sup> to design a catalyst that is effective under visible light<sup>5</sup>. The n-type semiconductor, ZnO has a wide band gap of 3.37 eV. It is low in toxicity and has excellent photocatalytic activity<sup>6</sup>. As a result, ZnO has a chance to have potential use in the future photoelectronic devices. However, only the UV light can cause excitation of electrons from valance band to conduction band of ZnO. In order to make ZnO effective under visible light, a number of techniques have been investigated, including ion doping<sup>7</sup>, noble metal deposition<sup>8</sup>, semiconductor coupling<sup>9</sup>, and surface sensitization<sup>10</sup>. Coupled with a semiconductor, high photocatalytic activities have been achieved in the majority of visible light regions. Several different types of inorganic semiconductor potential materials were investigated by Wadia et al.<sup>11-13</sup>. The researchers discovered several inorganic semiconductor photovoltaic materials, including FeS, Cu<sub>2</sub>S, Zn<sub>3</sub>P<sub>2</sub>, Cu<sub>2</sub>O, PbS etc. Therefore, V<sub>3</sub>O<sub>4</sub><sup>14</sup>, CuO<sup>15</sup>, and Cu<sub>2</sub>O<sup>16,17</sup> are examples of semiconductors that can be used for coupling. Cu<sub>2</sub>O is a type of conventional p-type semiconductor with a 2.1 eV band gap. In the visible light range, the absorption coefficient of Cu<sub>2</sub>O is high. However, because of photo-induced corrosion, it can also be quickly deactivated<sup>18</sup>. To avoid problems, two or more semiconductors are frequently mixed, or a semiconductor is merged with another material, for example, TiO<sub>2</sub>-Cu<sub>2</sub>O, WO<sub>3</sub>-TiO<sub>2</sub>, CeO<sub>2</sub>-ZnO, TiO<sub>2</sub>-ZnO, ZnO-Cu<sub>2</sub>O and so on<sup>19-24</sup>. The ZnO-Cu<sub>2</sub>O composite can improve visible light catalysis, which can reduce costs in real-life applications. The photocatalytic activity of various forms

\* Author of correspondence, e-mail: [mufazzal@du.ac.bd](mailto:mufazzal@du.ac.bd)

of Cu<sub>2</sub>O/Zn was explored under UV light by Wu et al<sup>25</sup>. In the present research, ZnO-Cu<sub>2</sub>O has been successfully prepared by precipitation followed by calcination. The composite is stable, inexpensive, and simple to prepare compared to materials made using other techniques. Most importantly the composite materials are effective photocatalyst under visible light.

## II. Experimental

### Preparation of ZnO-Cu<sub>2</sub>O composite

Cu(NO<sub>3</sub>)<sub>2</sub> solutions of different concentrations were mixed with different amounts of ZnO to prepare the composite of different compositions. Each suspension was sonicated for 30 minutes for better dispersion of solid ZnO. 0.50 M NaOH solution was then added drop wise into the suspension that was in constant and continuous stirring. After complete precipitation of Cu(OH)<sub>2</sub>, Fehling solution 2 containing sodium potassium tartrate and NaOH was added with constant stirring to produce a clear solution. 0.20 M glucose solution was added at 60 °C to prepare Cu<sub>2</sub>O precipitate. The stirring is continued to for another 30 minutes for formation of complete dark yellow precipitate. The precipitate is separated by decantation and washed several times with deionised water. Finally the prepared material was dried at 60 °C for 8 hours and stored in a desiccator.

### Characterization of prepared composite

The microstructure and structural morphology, the sample's elemental composition or chemical characterization, crystalline phases, chemical bonding nature and band gap energy were characterized by scanning electron microscopy (SEM), energy dispersive X-ray spectroscopy (EDX), X-ray diffractometer (XRD), Fourier transform infrared (FT-IR) spectroscopy and UV-visible reflectance measurement.

### Experimental set up for photodegradation

A 100.0 mL beaker was used as the reactor for all of the experiments. The source of radiation was visible light (380 nm-780 nm) in a wooden box. The distance between the solution surface and the radiation source was fixed, and the reactor was placed on a magnetic stirrer. Aluminium foil was used to cover the surfaces inside the box to avoid the absorption of light.

Visible light was shone upon the reaction mixture (MB and composite suspension). About 5.0 mL of the reaction mixture was collected in centrifuge tubes at different time intervals throughout the irradiation process and centrifuged in the centrifuge machine at a speed of 4500 rpm in order to get clear solution. The absorbance of the clear solution was measured at the  $\lambda_{\text{max}} = 664.5$  nm using UV-visible spectrophotometer. The photodegradation of MB solutions in the presence of UV and sunlight was carried out in the same beaker maintaining the same experimental conditions. The following formula has been used to calculate the percent degradation.

$$\% \text{ of degradation} = \frac{(A_0 - A)}{A_0} \times 100$$

= initial dye absorbance

A = dye absorbance after certain period of irradiation

## III. Result and Discussion

### SEM analysis of the prepared composite

The microstructure and surface morphology were determined by SEM. The SEM images of ZnO(A), Cu<sub>2</sub>O(B), and ZnO-Cu<sub>2</sub>O composite (C) are shown in Fig 1. The microstructure of commercial ZnO is shown with agglomerated nanoparticles and the particle sizes are irregular and non-uniform. On the other hand, the produced Cu<sub>2</sub>O is composed of homogeneous spherical nanoparticles with smaller particle size. The inclusion of Cu<sub>2</sub>O changes the particle size of ZnO. Consequently, composite nanoparticles are homogenous, uniform, and well-ordered.

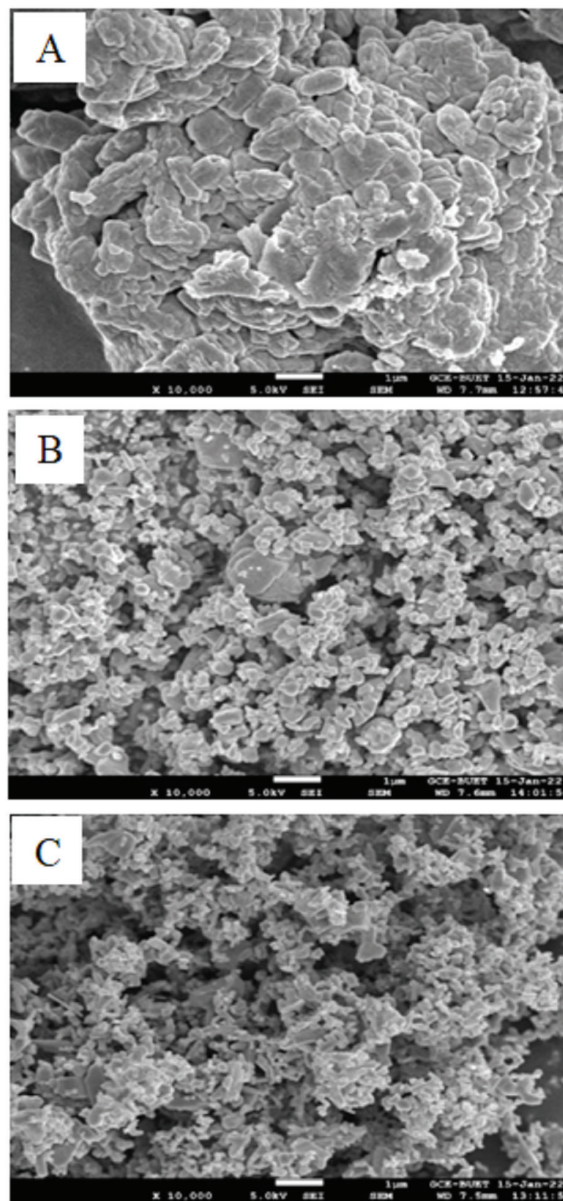


Fig. 1. The SEM images of commercial ZnO(A), Cu<sub>2</sub>O(B) and ZnO-Cu<sub>2</sub>O composite(C).

### EDX analysis of the prepared composite

The elemental composition of the sample or chemical characterization was done by EDX. Fig. 2 represents the EDX spectrum of commercial ZnO(A), Cu<sub>2</sub>O(B) and ZnO-Cu<sub>2</sub>O composite (C). Zinc and oxygen elements are found in ZnO whereas copper and oxygen are present in the prepared Cu<sub>2</sub>O. But the existence of zinc, copper, and oxygen is confirmed in ZnO-Cu<sub>2</sub>O nanocomposite through the EDX spectrum. It can be concluded that all of the samples are quite pure and no impurities are present.

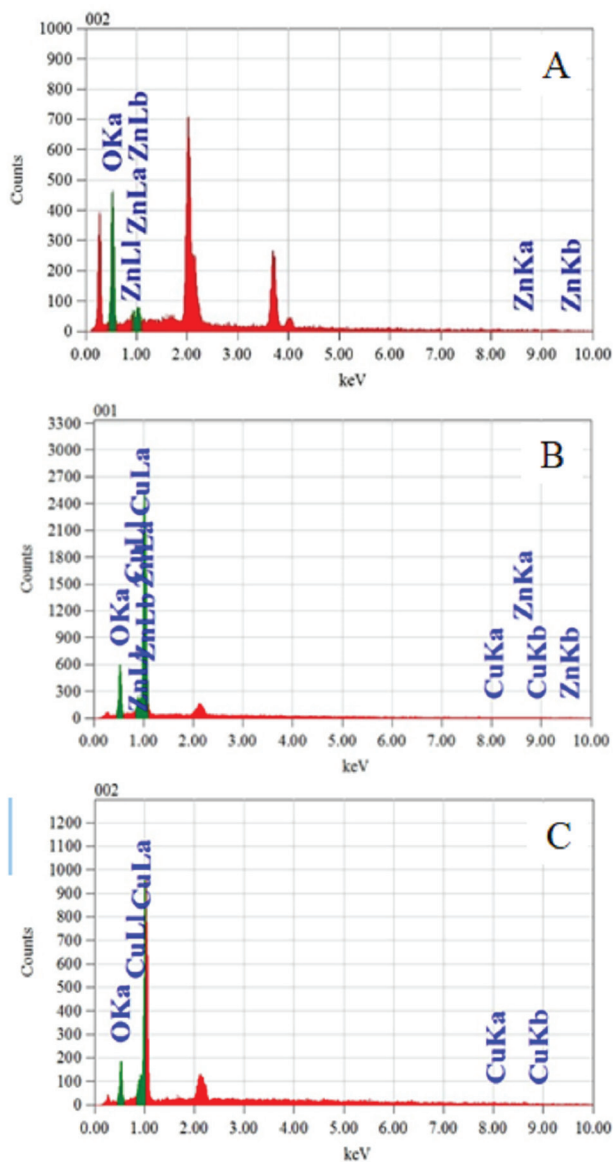


Fig. 2. The EDX spectrum of commercial ZnO(A), Cu<sub>2</sub>O(B) and ZnO-Cu<sub>2</sub>O composite(C).

### XRD analysis of the prepared composite

The X-Ray diffraction patterns of ZnO and ZnO-Cu<sub>2</sub>O composite were shown in Fig. 3. In commercial ZnO, peaks appear at  $2\theta = 31.750^\circ, 34.439^\circ, 36.251^\circ, 47.541^\circ, 56.553^\circ, 62.868^\circ, 66.386^\circ, 67.915^\circ, 69.055^\circ$  diffraction which

correspond to (100), (002), (101), (102), (110), (103), (200), (112), and (201) planes of the hexagonal wurtzite structure of ZnO according to the diffraction card JCPDS05-0664 ( $a=b=0.3249$  nm and  $c=0.5206$  nm)<sup>27</sup>. In this case, all of the peaks are exceedingly sharp which prove that the ZnO particles has a high crystallinity. The diffraction peaks in the XRD patterns of ZnO-Cu<sub>2</sub>O composite at  $2\theta$  value of

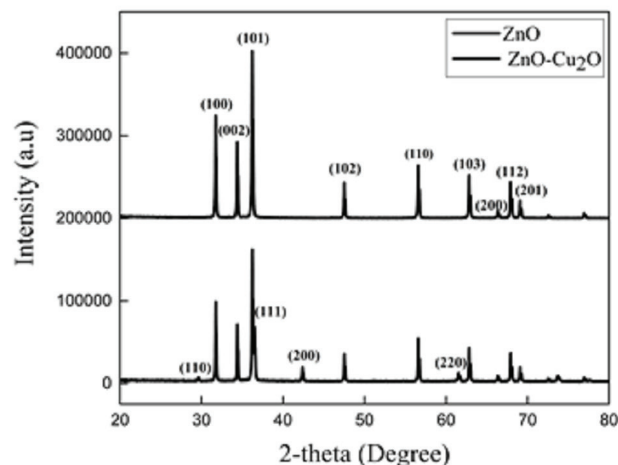


Fig. 3. The XRD patterns of commercial ZnO and the composite (ZnO:Cu<sub>2</sub>O = 90:10)

$29.554^\circ, 36.418^\circ, 42.297^\circ$  and  $61.344^\circ$  correspond to the reflection from (110), (111), (200) and (220) crystal planes of the cubic structure of Cu<sub>2</sub>O ( $a = b = c = 0.42696$  nm) which is in agreement with the diffraction card JCPDS05-0667<sup>28</sup>. In the composite, the crystallite size does not change significantly after doping and no peaks of any other phase or impurities such as CuO, Cu(OH)<sub>2</sub> and Zn(OH)<sub>2</sub> can be seen. Besides, in ZnO-Cu<sub>2</sub>O there is negligible displacement of the (103) peak of ZnO, which should indicate the presence of lattice interaction. The p-n heterojunction is the result of the lattice interaction. Thus, it may be concluded that the ZnO and Cu<sub>2</sub>O phases are coexist in the composite.

### FT-IR spectral analysis of the prepared composite

Fig. 4 shows the FTIR spectra of commercial ZnO, ZnO-Cu<sub>2</sub>O composite, and Cu<sub>2</sub>O. Despite the spectra was ran from 400 to 4000 cm<sup>-1</sup>, the bands from metal oxides are frequently below 1000 cm<sup>-1</sup><sup>29</sup>. The fundamental mode of vibration in the ZnO FT-IR spectrum shown in the Figure is O-H stretching at 3452.58 cm<sup>-1</sup>, which is related to water adsorption on the metal surface, respectively. C-H stretching vibration is shown at 2924.09 cm<sup>-1</sup>. Zn forms a tetrahedral coordination, which is the origin of the absorption at 875 cm<sup>-1</sup>. The anti-symmetric stretching vibrations of the O-Zn-O bonds in tetrahedral coordination are responsible for the band at 426.2 cm<sup>-1</sup>. The stretching vibration of Cu-O in Cu<sub>2</sub>O was attributed to the bands at 478.35, 628.79, and 1083.99 cm<sup>-1</sup>. The result has established the existence of Cu<sub>2</sub>O. There are no bands associated to CuO that would emerge at 588 and 534 cm<sup>-1</sup>. The peak at 430.13 and 630.13 cm<sup>-1</sup> in the composite are attributable to stretching vibrations of Zn-O and Cu-O,

respectively, indicating that ZnO and Cu<sub>2</sub>O are coexist in the ZnO-Cu<sub>2</sub>O composite.

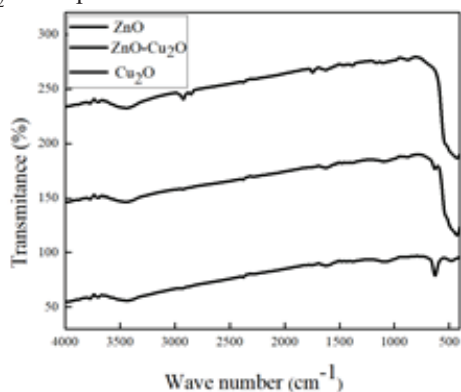


Fig. 4. The FT-IR spectra of the commercial ZnO, composite (ZnO:Cu<sub>2</sub>O = 90:10) and Cu<sub>2</sub>O

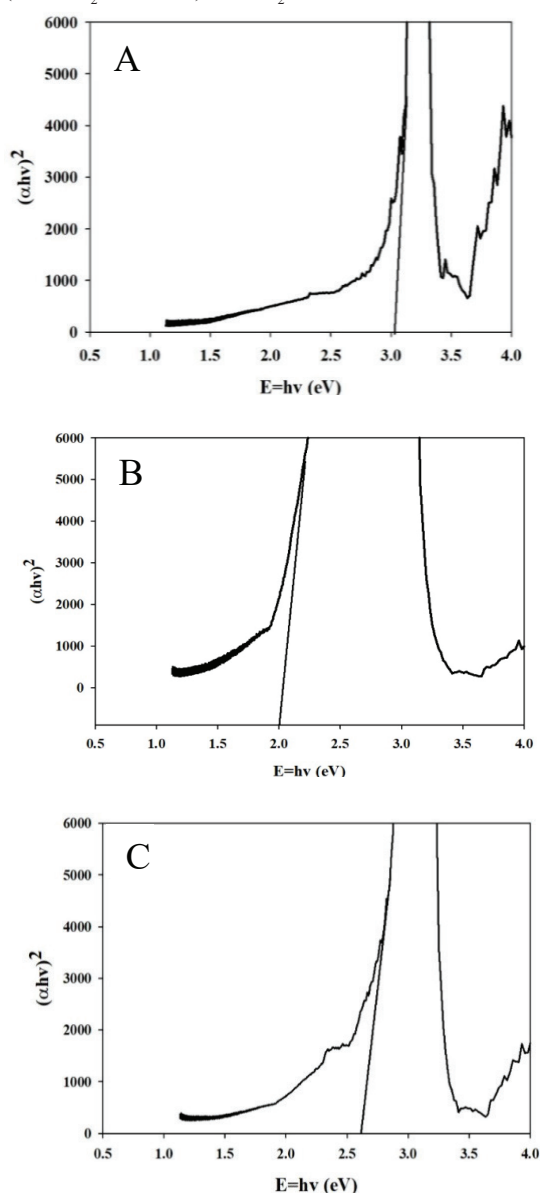


Fig. 5. Plots for the determination of band gap energy of ZnO(A), Cu<sub>2</sub>O(B) and ZnO-Cu<sub>2</sub>O composite(C).

#### Band gap energy determination

UV-vis diffuse reflectance spectroscopy was used to evaluate the samples' band gap energy. Fig. 5 represents the band gap energy of commercial ZnO, ZnO-Cu<sub>2</sub>O composite and prepared Cu<sub>2</sub>O. The bandgap energy of the nanocomposites can be determined by extrapolating the linear portion of the graph between the Kubelka-Munk function  $[F(R)hv]^2$  and the energy ( $E=hv$ ) of the nanocomposites. As shown in the Figure, ZnO, Cu<sub>2</sub>O and ZnO-Cu<sub>2</sub>O composite have band gap energies of 3.10, 2.00 and 2.64 eV respectively. In the composite, the creation of a p-n heterojunction between ZnO and Cu<sub>2</sub>O leads to a narrowing of the bandgap to the visible region. So, the prepared composite is expected to be a better photocatalyst because of its lower band gap energy.

#### Effect of composites with different molar ratio of ZnO and Cu<sub>2</sub>O on photodegradation of MB

To ascertain the impact of molar ratios of the composite on photodegradation of MB, a series of concurrent experiments were done using 0.30 g of composite of each ratio,  $3.0 \times 10^{-5}$  M concentration of MB under visible light. Fig. 6 shows the impact of the variation of molar ratios on the photodegradation of MB. The outcomes indicated that the composite of the ratio 90:10 showed the highest photocatalytic activity than the commercial ZnO or prepared Cu<sub>2</sub>O individually. The degradation efficiency of about 90.09% at 90 minutes of irradiation has been reported with this composite. In the composites, Cu<sub>2</sub>O may form electron-hole pairs due to its small bandgap energy by the visible light. The conduction band potential of Cu<sub>2</sub>O is more negative than that of ZnO. As a result the visible light induced photogenerated electron should be transferred from conduction band of Cu<sub>2</sub>O to that of ZnO preventing electron-hole recombination. At the same time, the interface between p-type semiconductor, Cu<sub>2</sub>O and n-type semiconductor, ZnO forms a p-n heterogeneous structure, which increases the transfer of photogenerated electron-hole pairs due to the potential energy difference. The overall result of all of these is an increase in the composite's photocatalytic activity.

Furthermore, the amount of ZnO required to produce the p-n heterojunction can be related to the higher photocatalytic activity. On the other hand, lower degradation efficiency was noticed for composites of the ratio with a lower ZnO content, as a small amount of p-n heterojunction is formed due to inadequate ZnO content in comparison to the composite of 90:10. Consequently, the composite of the molar ratio, ZnO:Cu<sub>2</sub>O = 90:10 has been used as a photocatalyst throughout the subsequent experiments.

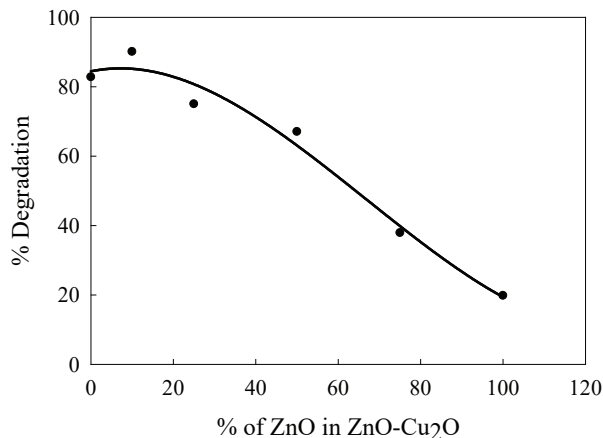


**Fig. 6.** Impact of various molar ratios on degradation of MB using composite and comparison with commercial ZnO and Cu<sub>2</sub>O (Prepared),  $[MB]_0 = 3.0 \times 10^{-5} M$ , composite amount = 0.30 g, initial pH =  $6.90 \pm 0.5$ .

#### *Effect of the amount of composite on photodegradation of MB*

To investigate the impact of amount of ZnO-Cu<sub>2</sub>O composite as a catalyst on the degradation of MB, a series of experiments were carried out by varying the amount of catalyst from 0.10-0.60g/100 mL with all other parameters maintaining constants ( $[MB]_0 = 3 \times 10^{-5} M$ , pH =  $6.90 \pm 0.5$ ) under visible light. Fig. 7 shows the effect the amount of catalyst on photodegradation of MB. It has been found that the degradation efficiency of MB increases from 77.30% to 98.94% with an increase in the amount of catalyst from 0.10 g to 0.40 g/100 mL. This can be explained by the presence of active sites on the catalyst surface, capability of photon absorption and the penetration of visible light into the suspension. The availability of a large number of active sites on the surface of the catalyst and the high photon absorption increase the formation of reactive OH<sup>•</sup> radicals and other reactive oxidative species (ROS).

As a result, the MB and ROS interact more frequently and effectively, accelerating the photodegradation. The optimum amount of catalyst for the highest photodegradation has been found to be 0.40 g/100 mL. A further increase in the amount of catalyst from 0.40 g to 0.60 g/100 mL decreases the degradation efficiency from 98.94% to 82.67%. This may be due to the scattering of the light and miniaturized the transmission of photon in the solution. Additionally, catalyst particles may agglomerate at higher concentrations, which may lower the number of active surface sites available for interaction between MB and catalyst. Additionally, at greater catalyst concentrations, some excited ZnO-Cu<sub>2</sub>O may interact with inactive catalyst and become deactivated, decelerating the photocatalytic degradation process<sup>30</sup>. On the other hand, 0.40 g of composite is taken as the optimum value for other subsequent photodegradation experiments.

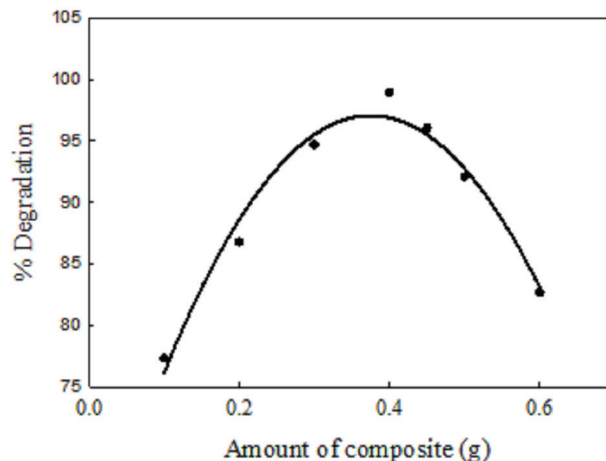


**Fig. 7.** Impact of composite amount on degradation of MB,  $[MB]_0 = 3.0 \times 10^{-5} M$ , initial pH =  $6.90 \pm 0.5$ , light source=visible light

#### *Impact of initial concentration of MB on photodegradation*

After optimizing the variables, i.e. molar ratio of the composite and the amount of catalyst, the photocatalytic degradation of MB was executed by changing the initial concentration of MB from  $3.8 \times 10^{-5} M$  to  $2.2 \times 10^{-5} M$  in order to obtain the optimum concentration for maximum degradation under visible light. Fig. 8 delineates the percent degradation with varying initial concentration of MB by using 0.40/100 mL ZnO-Cu<sub>2</sub>O composite of 90:10 ratio. It has been noticed that the percent of degradation decreases with the increase of the concentration of MB.

The reason for this is that a fixed amount of catalyst produces a fixed number of electron-hole pairs and OH<sup>•</sup> radicals, and these radicals can only degrade a given amount of MB. Besides, the percent degradation is calculated by dividing by the initial concentration term.

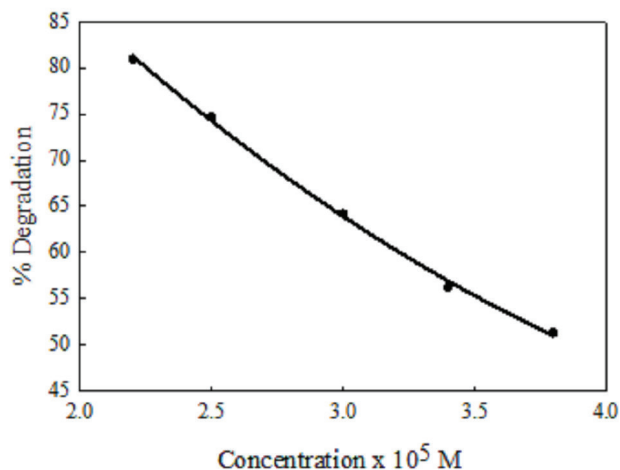


**Fig. 8.** Impact of initial concentrations of MB on degradation using the composite, composite amount (ZnO:Cu<sub>2</sub>O=90:10)=0.40 g, initial pH =  $6.90 \pm 0.5$ , light source=visible light.

Thus, it is most likely that percent degradation is lower when the initial dye concentration is higher. Additionally, a high dye concentration can make the light difficult to penetrate the bulk of the solution leading to decrease in hydroxyl radical formation and diminish of degradation efficiency. Thus, higher concentrations have an adverse influence on photodegradation.

#### IV. Conclusion

In the research work, the ZnO-Cu<sub>2</sub>O composites with various molar ratios have been prepared by precipitation followed by heating at 60°C temperature. The composite is characterized using SEM, EDX, FT-IR, XRD, and UV-visible reflectance measurement techniques. The SEM images show that the prepared composite has different particle size and morphology than the individual components. The band gap energy of the prepared composite is found to be between the values of commercial ZnO and Cu<sub>2</sub>O. The best MB degradation occurs with a ZnO-Cu<sub>2</sub>O composite of ratio of 90:10. The degradation of MB is carried out by varying the composite amount and initial concentration of MB. Most important result of this research is that the composite shows better activity under the visible light. Furthermore, this composite is prepared using commercial ZnO and prepared Cu<sub>2</sub>O by a cost-effective method. This technique can be used to remediate wastewater that contains textile dyes.

#### References

- Monika, K., 2012. Use of various technologies, methods and adsorbents for the removal of dye. *J. Environ. Res. Dev.*, **6** (3A), 879-883.
- Behnajady, M. A., N. Modirshahla, N. Daneshvar, and M. Rabbani, 2007. Photocatalytic degradation of an azo dye in a tubular continuous-flow photoreactor with immobilized TiO<sub>2</sub> on glass plates. *J. Chem. Eng.*, **127**(1-3), 167-176.
- Jonstrup, M., 2011. Treatment of textile waste waters using combination of biological and Physico-chemical methods. *J. Photochem. Photobiol. A: Chem*, **291**, 133-139.
- Islam, M. S., M. M. Hossain and T. S. Islam, 2010. Effect of pH, ions and ionic strength on TiO<sub>2</sub>-mediated photodegradation of brilliant orange. *Dhaka Univ. J. Sci.*, **58**, 187-190.
- Luo, J., Zhou X., Ma L., Xu. X., 2016. Rational construction of Z-scheme Ag<sub>2</sub>CrO<sub>4</sub>/g-C<sub>3</sub>N<sub>4</sub> composites with enhanced visible-light photocatalytic activity. *Appl. Surf. Sci.* **390**, 357-367.
- Ram, C., R. K. Pareek and V. Singh, 2012. Photocatalytic Degradation of Textile Dye by Using Titanium Dioxide Nanocatalyst. *Int. J. Theoretical and App. Sci.*, **4**(2), 82-88.
- Wang, X., Y. Sun, C. Liu, W. Feng, and D. Zou. 2015. Enhanced visible-active photochromism of a polyoxometalates/TiO<sub>2</sub> composite film by combining Bi<sub>2</sub>O<sub>3</sub> nanoparticles. *Rsc. Adv.* **5**, 49153-49158.
- Luo, J., X. Zhou, X. Ning, L. Zhan, L. Huang, Q. Cai, S. Li and S. Sun. 2018. Enhancing visible-light photocatalytic performance and stability of Ag<sub>3</sub>PO<sub>4</sub> nanoparticles by coupling with hierarchical flower-like In<sub>2</sub>S<sub>3</sub> microspheres. *Mater. Res. Bull.* **100**, 102-110.
- Luo, J., X. Zhou, X. Ning, L. Zhan, L. Ma, X. Xu, S. Li and S. Sun. 2018. Utilization of LaCoO<sub>3</sub> as an efficient co-catalyst to boost the visible light photocatalytic performance of g-C<sub>3</sub>N<sub>4</sub>. *Separation and Purification Technology.* **201**, 309-317.
- Dai, D., H. Xu, L. Ge, C. Han, Y. Gao, S. Li, and Y. Lu, 2017. In-situ synthesis of CoP co-catalyst decorated ZnO. 5Cd0. 5S photocatalysts with enhanced photocatalytic hydrogen production activity under visible light irradiation. *App. Catal. B: Environ.*, **217**, 429-436.
- Liu, X., Y. Yang, Y. Han, L. Wang, G. Chen, X. Xiao, and Wang, Y., 2017. H<sub>2</sub>O<sub>2</sub>-based green corrosion route to ZnO microrods photocatalysts on Zn plate. *J. Nanostructures*, **7**(1), 82-87
- Huang, Q., and J. Li, 2017. Enhanced photocatalytic and SERS properties of ZnO/Ag hierarchical multipods-shaped nanocomposites. *Mater. Lett.*, **204**, 85-88.
- Harish, S., J. Archana, M. Sabarinathan, M. Navaneethan, K. D. Nisha, S. Ponnusamy and Y. Hayakawa, 2017. Controlled structural and compositional characteristic of visible light active ZnO/CuO photocatalyst for the degradation of organic pollutant. *App. Surf. Sci.*, **418**, 103-112.
- Chava, R. K. and M. Kang, 2017. Ag<sub>2</sub>S quantum dot sensitized zinc oxide photoanodes for environment friendly photovoltaic devices. *Mater. Lett.*, **199**, 188-191.
- Wadia, C., A. P. Alivisatos, and D. M. Kammen, 2009. Materials availability expands the opportunity for large-scale photovoltaics deployment. *Env. Sci. Tech.*, **43**(6), 2072-2077.
- Luo, Y., L. Wang, Y. Zou, X. Sheng, L. Chang, and D. Yang, 2011. Electrochemically deposited Cu<sub>2</sub>O on TiO<sub>2</sub> nanorod arrays for photovoltaic application. *Electrochem. Solid-State Lett.*, **15**(2), H34.
- Herion, J., E. A. Niekisch and G. Scharl, 1980. Investigation of metal oxide/cuprous oxide heterojunction solar cells. *Solar Energy Mater.*, **4**(1), 101-112.
- Harish, S., M. Sabarinathan, J. Archana, M. Navaneethan, S. Ponnusamy, C. Muthamizhchelvan, and Y. Hayakawa, 2017. Functional properties and enhanced visible light photocatalytic performance of V<sub>2</sub>O<sub>4</sub> nanostructures decorated ZnO nanorods. *App. Surf. Sci.*, **418**, 171-178.
- Xu, L., Y. Zhou, Z. Wu, G. Zheng, J. He and Y. Zhou, 2017. Improved photocatalytic activity of nanocrystalline ZnO by coupling with CuO. *J. Phys. Chem. Solids*, **106**, 29-36.
- Adamu, H., A. J. McCue, R. S. Taylor, H. G. Manyar and J. A. Anderson, 2017. Simultaneous photocatalytic removal of nitrate and oxalic acid over Cu<sub>2</sub>O/TiO<sub>2</sub> and Cu<sub>2</sub>O/TiO<sub>2</sub>-AC composites. *App. Catal. B: Environ.*, **217**, 181-191.
- Huang, L., F. Peng, H. Yu, and H. Wang, 2009. Preparation of cuprous oxides with different sizes and their behaviors of adsorption, visible-light driven photocatalysis and photocorrosion. *Solid State Sci.*, **11**(1), 129-138.
- Xu, Y. H., D. H. Liang and D. Z. Liu, 2008. Preparation and characterization of Cu<sub>2</sub>O-TiO<sub>2</sub>: efficient photocatalytic degradation of methylene blue. *Mater. Res. Bull.*, **43**(12), 3474-3482.
- Han, C., Z. Li and J. Shen, 2009. Photocatalytic degradation of dodecyl-benzenesulfonate over TiO<sub>2</sub>-Cu<sub>2</sub>O under visible irradiation. *J. Hazard. Mater.*, **168**(1), 215-219.

24. Lu, G., X. Li, Z. Qu, Q. Zhao, H. Li, Y. Shen and G. Chen, 2010. Correlations of  $\text{WO}_3$  species and structure with the catalytic performance of the selective oxidation of cyclopentene to glutaraldehyde on  $\text{WO}_3/\text{TiO}_2$  catalysts. *J. Chem. Eng.*, **159(1-3)**, 242-246.
25. Chung, J. L., J. C. Chen and C. J. Tseng, 2008. Electrical and optical properties of  $\text{TiO}_2$ -doped ZnO films prepared by radio-frequency magnetron sputtering. *J. Phys. Chem. Solids*, **69(2-3)**, 535-539.
26. Shifu, C., Z. Wei, L. Wei, Z. Huaye and Y. Xiaoling, 2009. Preparation, characterization and activity evaluation of p-n junction photocatalyst p- $\text{CaFe}_2\text{O}_4/\text{n-ZnO}$ . *J. Chem. Eng.*, **155(1-2)**, 466-473.
27. He, T., Z. Zhou, W. Xu, Y. Cao, Z. Shi, and W. P. Pan, 2010. Visible-light photocatalytic activity of semiconductor composites supported by electrospun fiber. *Composites Sci. Tech.*, **70(10)**, 1469-1475.
28. Jiang, D., C. Xing, X. Liang, L. Shao and M. Chen, 2016. Synthesis of cuprous oxide with morphological evolution from truncated octahedral to spherical structures and their size and shape-dependent photocatalytic activities. *J. colloid and interface Sci.*, **461**, 25-31.
29. Saien, J., H. Delavari, and A. R. Solymani, 2010. Sono-assisted photocatalytic degradation of styrene-acrylic acid copolymer in aqueous media with nano titania particles and kinetic studies. *J. Hazardous Mater.*, **177(1-3)**, 1031-1038.
30. Gaim, Y. T., G. M. Tesfamariam, G. Y. Nigussie and M. E. Ashebir, 2019. Synthesis, Characterization and Photocatalytic Activity of N-doped  $\text{Cu}_2\text{O}/\text{ZnO}$  Nanocomposite on Degradation of Methyl Red. *J. Composites Sci.*, **3(4)**, 93.